A Systematic Design Approach for Non-coherent Grassmannian Constellations

Kareem M. Attiah*, Karim Seddik†, Ramy H. Gohary‡ and Halim Yanikomeroglu‡
*Department of Electrical Engineering, Alexandria University, Alexandria 21544, Egypt
†Electronics Engineering Department, American University in Cairo, AUC Avenue, New Cairo 11835, Egypt
‡Department of Systems and Computer Engineering, Carleton University, Ottawa, Canada

***Abstract*—In this paper, we develop a geometry-inspired methodology for generating systematic and structured Grassmannian constellations with large cardinalities. In the proposed methodology we begin with a small close-to-optimal "parent" Grassmann constellation. Each point in this constellation is augmented with a number of "children" points, which are generated along a set of geodesics emanating from that point. These geodesics are chosen to ensure close-to-maximal spacing. In particular, the directions of the geodesics and the distance that each "children" point is moved are chosen to maximize the pairwise Frobenius distance between the resulting constellation points. Although finding these directions directly seems difficult, by embedding the Grassmann manifold on a sphere of larger dimension, we were able to develop structures that are not only simple to generate but that also yield constellations that, under certain conditions, satisfy the maximum distance criterion and lie within a decaying gap from a tight upper bound. Numerical results suggest that the performance of the new constellations is comparable to that of the ones generated directly and significantly better than the performance of the ones generated using the exponential map.**

I. Introduction

Non-coherent multiple-input multiple-output (MIMO) communication systems are those systems in which neither the receiver nor the transmitter has access to channel state information (CSI). As such, these systems do not require the transmitter to waste valuable communication resources in order for the receiver to learn the channel. This feature of non-coherent systems renders them attractive for a variety of wireless communication systems, including the massive MIMO ones and those with bursty traffic which are likely to arise in the emerging area of Internet-of-Things. In fact, non-coherent systems have been identified by the European 2020 METIS project [1] as one of the enablers of the prospective 5G cellular networks.

Unfortunately, in the general case the rate-optimal non-coherent signaling over block-fading channels is still an open problem. However, at asymptotically high signal-to-noise ratios (SNRs), the signals that approach capacity were shown in [2] to be in the form of matrices that span isotropically distributed points on the so-called compact Grassmann manifold, that is, the set comprising the subspaces spanned by all unitary matrices with certain dimensions. Several approaches for designing non-coherent constellations have been explored in the literature. These approaches can be classified into two main categories.

In the first category, the Grassmannian constellation is designed based on information-theoritic arguments, which amount to maximizing various pairwise distance metrics between constellation points [3], [4]. In particular, in this category the constellation design is formulated as a sphere-packing problem on the Grassmann manifold, which is known to constitute a formidable task even in a spaces with less intricate structures. Using numerical optimization approaches, several 'good' constellation were generated, see e.g., [3] and [4]. However, this approach suffers from a number of drawbacks: first, constellations designed with this approach do not possess a particular structure that can facilitate their detection; second, since Grassmannian constellations are desirable for high SNR operation, the cardinality of these constellations is usually very high, which renders their storage and manipulation rather unwieldy [2]; and finally, the computational cost of generating constellations with unitarity constraints is generally high even for relatively small constellations. Hence, it can be seen that, despite the performance advantage of Grassmannian constellations generated with numerical techniques, the practicality of these constellations is rather questionable.

In the second category, the constellations are generated using algebraic constructions [5] or paramterized mappings [6], [7]. In contrast with the constellations generated using the numerical approach, these constructions offer significant advantages in design simplicity and detection complexity. Unfortunately, however, the stringent construction of these constellations limits their flexibility and often results in heavy performance losses.

Having discussed the two main philosophies for designing Grassmannian constellations, in this paper we seek to combine the design and detection simplicity of algebraically-designed constellations with the performance advantages of numerically-designed ones. In order to do so, we introduce a structured approach that facilitates the design of the constellations while maintaining distance profiles similar to those reported in [3] and [4]. In particular, in this approach we begin by designing an initial low-cardinality "parent" constellation. Each point of this constellation is then augmented with a number of "children" points. The children points are distanced from their respective parent points along geodesics emanating from the parent points in specific directions, which are determined algebraically. Finally, the scalar distance that each point travels away from its parent point is optimized numerically. Hence, it can be seen that this approach indeed combines the design efficiency of algebraically-design constellations with the flexibility offered by numerical optimization. Numerical simulations show that the constellations generated with the

proposed approach exhibit a performance superior to that of the constellations generated with the pure algebraic approach in [7] and comparable to the performance of the of the constellations generated with the pure numerical approach in [3]. In addition, the structure that underlies the new constellation renders them amenable to a sequential detection scheme. However, this scheme is not presented due to space limitations.

II. Preliminaries and System Model

A. The Grassmann Manifold

Consider two unitary matrices $\mathbf{P}, \mathbf{Q} \in \mathbb{C}^{T\times M}$, where $T > M$. The set containing all such matrices is known as the Stiefel manifold and for this manifold an equivalence relation can be defined whereby $\mathbf{P} \sim \mathbf{Q}$ if and only if a unitary matrix $\mathbf{\Xi} \in \mathbb{U}_M$ exists such that

$$\mathbf{P} = \mathbf{Q}\mathbf{\Xi}, \qquad \mathbf{\Xi} \in \mathbb{U}_M, \tag{1}$$

where $\mathbb{U}_M$ is the unitary group comprising all $M \times M$ unitary matrices with entries satisfying $\mathbf{\Xi}\mathbf{\Xi}^\dagger = \mathbf{\Xi}^\dagger\mathbf{\Xi} = \mathbf{I}_M$, where $\mathbf{I}_M$ is the $M \times M$ identity matrix.

Using the equivalence relation, the Grassmann manifold $\mathbb{G}_{T,M}(\mathbb{C})$ can be readily expressed as the quotient space of the set of $T \times M$ unitary matrices with respect to this equivalence relation. In other words, it is the set of all M dimensional subspaces in $\mathbb{C}^T$.

Using differential-geometric methods, the equation of motion on the Grassmann manifold was obtained in [8]. This equation describes the motion of a point, which at time $t = 0$, is located at $\mathbf{X}(0) = \mathbf{X} \in \mathbb{G}_{T,M}(\mathbb{C})$. When this point moves along a geodesic in the direction $\dot{\mathbf{X}}(0) = \mathbf{H} = \mathbf{X}_\perp\mathbf{B}$ for some $(T - M) \times M$ complex arbitrary matrix $\mathbf{B}$, its location at an arbitrary time instant t can be expressed as

$$\mathbf{X}(t) = [\mathbf{X} \quad \mathbf{X}_\perp] \exp\left(t \begin{bmatrix} 0 & -\mathbf{B}^\dagger \\ \mathbf{B} & 0 \end{bmatrix}\right) \mathbf{I}_{T,M}, \tag{2}$$

where $\mathbf{X}_\perp$ is the $T \times (T - M)$ orthogonal complement of $\mathbf{X}$ in the $T \times T$ complex Euclidean space and $\mathbf{I}_{T,M} = [\mathbf{I}_M \quad \mathbf{0}]^\dagger$; i.e., $\mathbf{I}_{T,M}$ is obtained from $\mathbf{I}_T$ by keeping its first M columns and truncating the remaining $T - M$ columns. The notation $\mathbf{B}^\dagger$ denotes the Hermitian transpose of the matrix $\mathbf{B}$.

In order to gain insight into the effect of the matrix $\mathbf{B}$ on the equation of motion, we consider its compact singular value decomposition, $\mathbf{B} = \mathbf{U}\mathbf{\Sigma}\mathbf{V}^\dagger$. Substituting this decomposition in (2) and simplifying yield the following equivalent representation thereof [8]:

$$\mathbf{X}(t) = g(\mathbf{X}, \mathbf{V}, \mathbf{U}, \mathbf{\Sigma}, t), \tag{3}$$

where

$$g(\mathbf{X}, \mathbf{V}, \mathbf{U}, \mathbf{\Sigma}, t) := [\mathbf{X} \quad \mathbf{X}_\perp] \begin{bmatrix} \mathbf{V}\cos\mathbf{\Sigma}t \\ \mathbf{U}\sin\mathbf{\Sigma}t \end{bmatrix}. \tag{4}$$

We will find the expression in (3) more convenient than the one in (2) in revealing the roles of t, $\mathbf{U}$, $\mathbf{\Sigma}$ and $\mathbf{V}$.

B. System Model

We consider the frequency flat Rayleigh fading model in [2]. In this model the channel coefficients are assumed to remain essentially fixed during each channel coherence interval of T symbol durations, but to take on a statistically-independent realization in each of the subsequent coherence intervals. In our system, the numbers of transmit and receive antennas are denoted by M and N, respectively. Using this notation, the $T \times N$ received signal $\mathbf{Y}$ at a given coherence interval can be expressed as

$$\mathbf{Y} = \mathbf{X}\mathbf{H} + \sqrt{M/\gamma T}\,\mathbf{W}, \tag{5}$$

where $\mathbf{X}$ is the complex $T \times M$ unitary transmitted matrix, $\mathbf{H}$ is the $M \times N$ fading matrix whose coefficients are independent, identically distributed (i.i.d) drawn from the standard complex Gaussian distribution $\mathcal{CN}(0, 1)$, $\mathbf{W}$ is the $T \times N$ noise matrix which is also modeled as i.i.d complex Gaussian whose elements are $\mathcal{CN}(0, 1)$ and γ is the SNR. We consider the case of $N \geq M$ and $T \geq 2M$ throughout this paper.

C. Projection Frobenius Norm

The distance between two points on $\mathbb{G}_{T,M}(\mathbb{C})$ can be measured in several senses, and choosing an appropriate sense is crucial for designing 'good' Grassmannian constellations. In [2] and [3], it was argued that the design of capacity-approaching Grassmannian constellation ought to be guided by the sense in which noise perturbs the subspace that is spanned by the transmitted constellation point.

Other distance metrics for designing Grassmannian constellations have been proposed, cf. [4], [9]. The most common metric, and the one that we adopt herein, is the projection Frobenius distance (or simply the Frobenius distance). For any two points on the manifold $\mathbf{X}_i, \mathbf{X}_j \in \mathbb{G}_{T,M}(\mathbb{C})$ the Frobenius distance is given by

$$d(\mathbf{X}_i, \mathbf{X}_j) = \frac{1}{\sqrt{2}}\|\mathbf{X}_i\mathbf{X}_i^\dagger - \mathbf{X}_j\mathbf{X_j}^\dagger\|_F = \sqrt{M - \|\mathbf{X}_i^\dagger\mathbf{X}_j\|_F^2}. \tag{6}$$

Although there are other metrics that one would consider for designing non-coherent constellations, the Frobenius distance avoids singularity issues that complicate the design [10]. In addition, this metric facilitates drawing insight into the structure of the Grassmann manifold. In particular, this metric corresponds to embedding $\mathbb{G}_{T,M}(\mathbb{C})$ in the space of $T \times T$ matrices of rank M. In this space, points on $\mathbb{G}_{T,M}(\mathbb{C})$ are uniquely mapped to points on a sphere of $T^2 - 1$ real dimensions, and these points are represented by their projection matrices [9], [10]. This fact will be exploited in the next section to develop a simple method for selecting good directions for generating the "children" constellation from the "parent" one.

III. Design Strategy

We now describe our approach in detail. Given an initial constellation ξ_1, we define a sequence of $L - 1$ sub-constellations (layers) $\xi_2, \ldots, \xi_L$, where each layer is obtained from previous layers via geodesic transitions on the manifold. In particular, consider the i^{th} "parent" layer $\mathcal{C}_i = \bigcup_{j=1}^{i-1} \xi_j$. Members of ξ_i are placed along K geodesics emanating from

each member in that parent layer. Formally speaking, for $i = 2, \ldots, L$ and $k = 1, \ldots, K$, ξ_i is obtained as

$$\xi_i = \{\mathbf{X}_k(t_i) : \mathbf{X}_k(t_i) = g(\mathbf{Z}, \mathbf{V}_k, \mathbf{U}_k, \mathbf{\Sigma}_k, t_i), \mathbf{Z} \in \mathcal{C}_i\}. \quad (7)$$

Observe that the step parameter t_i controls the distances at which the children points (i.e. members of ξ_i) lie from their respective parent points. The assumption here is that t_i is the same for all members of a given layer, but can be different from one layer to the next.

Finally, the union set comprising these L layer forms our constellation, $\mathcal{C} = \{\mathbf{X} : \mathbf{X} \in \bigcup_{i=1,\ldots,L} \xi_i\}$. The size of the constellation is given by $|\mathcal{C}| = N'(K+1)^{L-1}$, where N' is the initial constellation size. The criteria for constructing the initial constellation and the geodesic directions are given next.

A. Starting constellation

The initial constellation is constructed using the technique developed in [9] for packing spheres on $\mathbb{G}_{T,M}(\mathbb{C})$. We briefly review this algorithm: first, for a chosen arrangement of N' points on the Grassmannian $\{\mathbf{Q}_i\}_{i=1}^{N'}$, define the Gram matrix $\mathbf{G} = \mathbf{Q}^\dagger\mathbf{Q}$, where $\mathbf{Q} = [\mathbf{Q}_1, \ldots, \mathbf{Q}_{N'}]$. When the packing distance, d_{pack}, is greater than or equal to some number ρ, the matrix $\mathbf{Q}$ possesses certain structural and spectral properties. To exploit this observation, the algorithm in [9] initially selects a random arrangement of points and updates its Gram matrix by alternate enforcement of these properties for a distance $\rho = d_{opt} - \epsilon$, where d_{opt} is the optimal packing distance and ϵ is some positive small number. It follows that finding a Gram matrix that satisfies these properties yields a near-optimal arrangement of N' points on $\mathbb{G}_{T,M}(\mathbb{C})$.

This scheme extends for a number of metrics while the underlying algorithm remains the same. In this paper, this algorithm is used to build initial constellations with the Frobenius distance being the design metric. The above method is suitable for packing on the Grassmann manifold when the constellation size is small. Specifically, under such circumstances, it leads to packing arrangements whose packing diameter is close to known bounds. For our purposes, this is convenient since our choice of the initial constellation is typically small.

B. Choice of geodesic directions

To determine the geodesic directions, we will use the same metric as the one that was used in designing the initial constellation. For simplicity, we assume a constellation in which only two layers are incorporated (we will consider the general case later in this section).

Assuming that the design of the initial constellation is close to optimal in the sense of the Frobenius distance, we make the following observation: for small step sizes, the probability of detection error is dominated by the distances among children points associated with the same parent as well as their distances from that parent. The distance between a child and its parent is solely determined by the product $\mathbf{\Sigma}t$ and is therefore independent of the orientation of the geodesics along which children points are obtained (i.e., children geodesics). Thus, the orientations of the children geodesics, which are controlled by the triplets $\{\mathbf{V}_k, \mathbf{U}_k, \mathbf{\Sigma}_k\}_{k=1}^K$, only influence the inter-children distances. But, to exhibit good performance, our constellations need to maximize these distances.

Based on the above discussion, we propose that the directions of the children geodesics are to be chosen so as to maximize the inter-children distances for any step parameter t. Therefore, the determination of these directions can be obtained by solving the following optimization problem.

$$\begin{aligned} \max_{\{\mathbf{V}_k, \mathbf{U}_k, \mathbf{\Sigma}_k\}_{k=1}^K} \min_{i,j,i\neq j} \quad & d^2(\mathbf{X}_i(t), \mathbf{X}_j(t)) \\ \text{subject to } \mathbf{X}_k(t) &= \begin{bmatrix}\mathbf{Z} & \mathbf{Z}_\perp\end{bmatrix} \begin{bmatrix}\mathbf{V}_k \cos \mathbf{\Sigma}_k t \\ \mathbf{U}_k \sin \mathbf{\Sigma}_k t\end{bmatrix} \\ & d^2(\mathbf{X}_m(t), \mathbf{Z}) = d^2(\mathbf{X}_n(t), \mathbf{Z}),\ m \neq n,\ t \in \mathbb{R}. \end{aligned} \quad (8)$$

One may identify this problem as a packing problem on the Grassmannian in which we additionally require the children points be at the same distance from an initial point $\mathbf{Z} \in \xi_1$ and for any choice of t. To the best of our knowledge, this problem is generally intractable. We are unaware of a method of applying this criterion as it stands.

It is helpful at this point to visualize how the children geodesics that achieve maximum distance criterion look like in lower dimensions. This will be our starting point towards obtaining a simple structure that agrees, to a great extent, with the inherently optimal arrangement satisfying the previous problem. Consider the sphere shown in Fig. 1. It was shown in [10] that the Grassmann manifold with the projection Frobenius distance can be isometrically embedded on a sphere of dimension $D = T^2 - 1$ in which every point $\mathbf{X} \in \mathbb{G}_{T,M}(\mathbb{C})$ is represented by its projection matrices $\mathbf{X}\mathbf{X}^\dagger$. In that case, geodesics on $\mathbb{G}_{T,M}(\mathbb{C})$ are mapped into geodesics on that sphere. The chordal distance between Gramssmannian points is $1/\sqrt{2}$ times the straight line distance between the corresponding projection matrices.

In Fig. 1, the point $\mathbf{Z}\mathbf{Z}^\dagger$ represents some parent point. Naturally, children geodesics defined by optimal directions will also remain optimal when viewed on the sphere. The solid bold curves mark such geodesics. The "slices" A and B represent spheres of lower dimension whose points lie at distances d_1 and d_2, respectively, from $\mathbf{Z}$. Children points at the given distances are simply defined by intersection points of the optimal children geodesics and the spheres A, B. From the geometry of the figure, one can readily conclude that the optimal directions for the chosen geodesics remain optimal regardless of how far we step away from $\mathbf{Z}$. That is to say that the components associated with the directions of the geodesics in (3) and the distance at which the children lie can be treated independently. This observation suggests that $\mathbf{\Sigma}_1 = \mathbf{\Sigma}_2 = \cdots = \mathbf{\Sigma}_K = c\mathbf{I}_M$ for some constant c. Indeed, if, for some k, $\mathbf{\Sigma}_k \neq c\mathbf{I}_M$, then the incremental displacement of $\mathbf{X}_k(t)$ to a new point $\mathbf{X}_k(t')$, where $t' = t + \Delta t$ yields

$$\mathbf{X}_k(t') = [\mathbf{Z} \quad \mathbf{Z}_\perp] \begin{bmatrix}\mathbf{V} & 0 \\ 0 & \mathbf{U}\end{bmatrix} \begin{bmatrix}\cos \mathbf{\Sigma}\Delta t & -\sin \mathbf{\Sigma}\Delta t \\ \sin \mathbf{\Sigma}\Delta t & \cos \mathbf{\Sigma}\Delta t\end{bmatrix} \begin{bmatrix}\cos \mathbf{\Sigma}t \\ \sin \mathbf{\Sigma}t\end{bmatrix},$$

which clearly leads to a change in orientation as well.

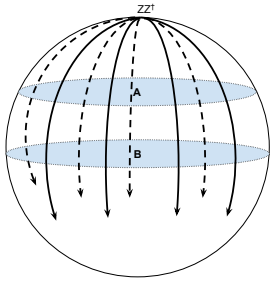

Fig. 1. Viewing the optimal directions in lower dimension as induced by geometric embedding of $\mathbb{G}_{T,M}(\mathbb{C})$ on a sphere.

Further, we also note that rotations in the geodesic directions do not disturb their optimality. Referring back to Fig. 1, the dotted curves are readily obtained by rotating the solid ones. One can quickly notice that such rotation does not modify the parent-child distance, nor does it affect the inter-children distances and therefore the new geodesics are also optimal.

Now that we have identified several features for the maximum distance criterion geodesics, we are in a position to explore our proposed arrangement. But before we introduce this structure, we review the following theorem that will help assess our proposed choice of the children geodesics. This theorem provides an upper bound on the packing distance. This bound was initially developed in [10] for real Grassmann manifolds, and was later generalized for $\mathbb{G}_{T,M}(\mathbb{C})$ in [9].

Theorem 1: The upper bound on the *unconstrained* problem in (8) is given by

$$\min_{i,j,i\neq j} d^2(\mathbf{X}_i(t),\mathbf{X}_j(t)) \leq \frac{M(T-M)}{T}\frac{K}{K-1}. \qquad (9)$$

This bound is achieved only when $K \leq \frac{T(T+1)}{2}$ for real Grassmannian, and $K \leq T^2$ for complex Grassmannian.

This bound was actually obtained by applying the principles due to Rankin for sphere packing in Euclidean spaces [11], [12] after embedding $\mathbb{G}_{T,M}(\mathbb{C})$ on a sphere. We will refer to this bound as the Rankin bound of Grassmannian packing.

We are now ready to present the following theorem.

Theorem 2: Let $T = 2M$, then setting $\mathbf{\Sigma}_1 = \mathbf{\Sigma}_2 = \cdots = \mathbf{\Sigma}_K = c\mathbf{I}_M$, $ct = \frac{\pi}{4}$, $\mathbf{U}_1 = \mathbf{U}_2 = \cdots = \mathbf{U}_K = \mathbf{U}$, and

$$(\mathbf{V}_1,\ldots,\mathbf{V}_K) = \arg \max_{\{(\tilde{\mathbf{V}}_1,\ldots,\tilde{\mathbf{V}}_K)|\tilde{\mathbf{V}}_k\in\mathbb{U}_M\}} \min_{i,j,i\neq j} \|\tilde{\mathbf{V}}_i - \tilde{\mathbf{V}}_j\|_F^2, \qquad (10)$$

achieves Rankin bound of packing on the Grassmannian, when $K \leq 2M^2+1$. Further, if $2M^2+1 \leq K \leq 4M^2$ the gap from that bound is not any greater than $\frac{M}{2}(\frac{K}{K-1}-1)$. Additionally, the orthogonal components $\{\mathbf{V}_k\}_{k=1}^K$ and the product ct can be chosen independently. In other words, $\{\mathbf{V}_k\}_{k=1}^K$ that satisfy the previous expressions are optimal for any ct.

Proof: See the Appendix. ∎

Having taken a look at Theorem 2, we can draw a number of consequences. First, not only is the Rankin bound achieved for number of directions smaller than $2M^2+1$ but it also ensures that the gap from optimality bound decreases with the number of directions when $2M^2+1 \leq K \leq 4M^2$.

Second, as the theorem points out, the choice of ct is completely transparent to $\{\mathbf{V}_k\}_{k=1}^K$. As long as $\{\mathbf{V}_k\}_{k=1}^K$ satisfy (10), the product ct can be chosen with absolute freedom. This is exactly what our geometric analysis suggested. This also implies that a multi-layer criterion in which only the step parameter is changed from one layer to another is possible. This ensures that our design adheres to several practical considerations regarding memory limitations, even when a large number of layers is incorporated. Finally, observe that Theorem 2 sets no restrictions whatsoever upon the unitary component $\mathbf{U}$. A question that arises is: in what manner should we select $\mathbf{U}$? For small constellations, $\mathbf{U}$ can indeed be chosen in an arbitrary manner; the natural choice is therefore $\mathbf{I}_{T-M,M}$. However, high rate scenarios are often characterized by overcrowded constellations, which are limited not only by the distances among children of common parents but also among those of different parents. Under such scenarios, it becomes essential to provide additional flexibility on the latter distances by changing $\mathbf{U}$ from one layer to the next.

The extension of Theorem 2 for $T > 2M$ is straightforward and is omitted for space limitations. The $\{\mathbf{V}_k\}_{k=1}^K$ that solve (10) can be obtained by first expressing the optimization problem in the following form

$$\min_{\{(\tilde{\mathbf{V}}_1,\ldots,\tilde{\mathbf{V}}_K)|\tilde{\mathbf{V}}_k\in\mathbb{U}_M\}} \max_{i,j,i\neq j} \operatorname{Tr}\tilde{\mathbf{V}}_i^\dagger\tilde{\mathbf{V}}_j + \operatorname{Tr}\tilde{\mathbf{V}}_j^\dagger\tilde{\mathbf{V}}_i \qquad (11)$$

where $\operatorname{Tr}(.)$ is the trace operator. Using the Jacobian approximation, $\max(a,b) \approx \log(\mathrm{e}^a + \mathrm{e}^b)$ for sufficiently large values of $|a-b|$, we obtain a smooth representation of (11) as follows.

$$\min_{\{(\tilde{\mathbf{V}}_1,\ldots,\tilde{\mathbf{V}}_K)|\tilde{\mathbf{V}}_k\in\mathbb{U}_M\}} \log \sum_{i,j,i\neq j} \mathrm{e}^{\operatorname{Tr}\tilde{\mathbf{V}}_i^\dagger\tilde{\mathbf{V}}_j + \operatorname{Tr}\tilde{\mathbf{V}}_j^\dagger\tilde{\mathbf{V}}_i}. \qquad (12)$$

In [8], generalized versions of conjugate gradient and Netwon's methods for orthogonal manifolds were developed. To solve (12), we have used the conjugate gradient method.

IV. RESULTS

In this section, we will assess the performance of our proposed scheme. To this end, we will compare our constellations to the direct ones in [3] and the exponential ones in [7]. In all simulations, we use $T = 4$, $N = M = 2$. For our method, two constellations are considered, which are denoted by $\mathcal{C}_1$ and $\mathcal{C}_2$. The starting constellation is of size $N' = 16$, which is the same for both constellations. In addition, we choose $K = 15$. Note that $2M^2+1 \leq K \leq 4M^2$ and the gap from optimality is at most 0.0714. The constellation $\mathcal{C}_1$ is bi-layered of size $N'(K+1) = 256$, while $\mathcal{C}_2$ is tri-layered of size $N'(K+1)^2 = 4096$. This corresponds to rates 2 and 3 bits per channel use (bpcu). For $\mathcal{C}_1$, we have chosen $\mathbf{U} = \mathbf{I}_2$ and $r_2 = 0.5$, where r_j is the ratio of the distance between a child in layer j and its respective parent to the starting constellation packing diameter. For $\mathcal{C}_2$, we have selected $\mathbf{U}_1 = \mathbf{I}_2$ and $r_2 = 0.6$ for the first children layer and $\mathbf{U}_2 = \begin{bmatrix} 0 & 1 \\ 1 & 0 \end{bmatrix}$ and $r_3 = 0.35$ for the second children layer. Finally, for comparison, we use the coherent constellation [7]

$$\mathbf{P} = \begin{bmatrix} s_1 + \theta s_2 & \phi(s_3 + \theta s_4) \\ \phi(s_3 - \theta s_4) & s_1 - \theta s_2 \end{bmatrix}, \qquad (13)$$

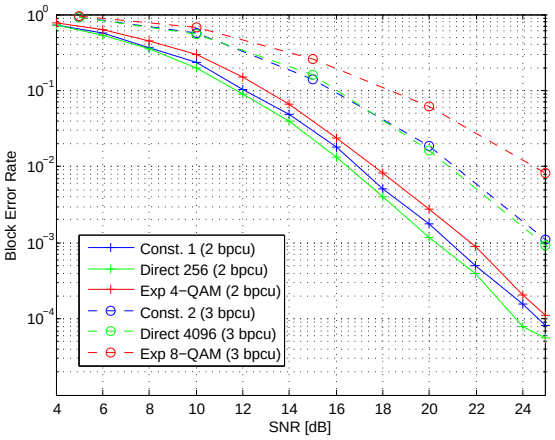

Fig. 2. Our constellations against the ones in [3] and [7], which are legened by "Direct" and "Exp", respectively.

where $\phi^2 = \theta = \mathrm{e}^{i\frac{\pi}{4}}$ and $s_j, j = 1, \ldots, 4$ are either 4-QAM with homothetic factor $\alpha = 0.3$, or 8-QAM symbols with homothetic factor $\alpha = 0.375$.

In Fig. 2, we plot the block error rates for $\mathcal{C}_1$ and $\mathcal{C}_2$ against the indicated constellations in [3], [7]. In this case, all constellations are decoded via the GLRT detector [13]. We see that our design outperforms the family of exponential mapping under different rate scenarios. Moreover, we also notice that the loss relative to the direct approach is acceptable.

V. Conclusion

In this paper, we propose a systematic approach for designing non-coherent space-time constellations over the Grassmann manifold. This approach can be used to generate large constellations with performance that is comparable to that of the best available constellations, but with significantly less design complexity and storage requirements. The new constellations are amenable to techniques that exploit their underlying structure to enhance detection efficiency.

Appendix

We first introduce the following lemma.

Lemma 1: Let

$$\beta = \min_{i,j,i\neq j} \|\tilde{\mathbf{V}}_i - \tilde{\mathbf{V}}_j\|_F^2, \tag{14}$$

for some $\tilde{\mathbf{V}}_k \in \mathbb{U}_M, k = 1, \ldots, K$. The following upper bounds hold on β.

1) If $K \leq 2M^2 + 1$, then $\beta \leq \frac{2MK}{K-1}$.
2) If $2M^2 + 1 \leq K \leq 4M^2$, then $\beta \leq 2M$.

Proof: Write

$$\|\tilde{\mathbf{V}}_i - \tilde{\mathbf{V}}_j\|_F^2 = \|\operatorname{vec}(\tilde{\mathbf{V}}_i) - \operatorname{vec}(\tilde{\mathbf{V}}_j)\|_2^2, \tag{15}$$

where $\operatorname{vec}(.)$ is an operator that lists out the entries of a matrix in a vector format. We then deduce that $\{\tilde{\mathbf{V}}_k\}_{k=1}^K$ form a spherical code $\mathcal{C}_s$ of cardinality $|\mathcal{C}_s| = K$ and squared radius $\rho = \|\tilde{\mathbf{V}}_i\|_F^2 = M$ which lies in an ambient space of $D = 2M^2$ real dimensions. The proof of the lemma then follows from applying Rankin principles in [11], [12]. ∎

We will now use this lemma to show the desired result. Consider the problem in (8), the constraints automatically hold since, for $i = 1, 2, \ldots, K$, we have

$$\begin{aligned} d^2(\mathbf{X}_i, \mathbf{Z}) &= M - \|\mathbf{Z}^\dagger \mathbf{X}_i\|_F^2 = M - \|\cos \mathbf{\Sigma} t\|_F^2 \\ &= M - M\cos^2 ct = M \sin^2 ct. \end{aligned}$$

Define $\sigma_{i,j} = d^2(\mathbf{X}_i(t), \mathbf{X}_j(t))$ and $\alpha_t = \cos(ct)$, using the proposed structure yields $\sigma_{i,j} = \alpha_t^2(1-\alpha_t^2)\|\mathbf{V}_i - \mathbf{V}_j\|_F^2$. Consequently, the problem in (8) reduces to

$$\left(\max_{\alpha_t} \quad \alpha_t^2(1-\alpha_t^2)\right)\left(\max_{\{\mathbf{V}_k \in \mathbb{U}_M\}_{k=1}^K} \min_{i,j,i\neq j} \|\mathbf{V}_i - \mathbf{V}_j\|_F^2\right). \tag{16}$$

One can now easily see that the orthogonal components and the step parameter can be independently optimized. Additionally, we observe that the orthogonal components remain optimal as long as they form a solution to the second problem in (16), irrespective of the value of α_t.

To show optimality, we notice that optimal value for the first problem in (16) is attained at $\alpha_t = \frac{1}{\sqrt{2}}$; in which case the optimal value is $\frac{1}{4}$. For the second problem, the optimal value follows from Lemma 1, and is attainable when $K \leq 2M^2+1$. We conclude that (16) is upper bounded by $\frac{MK}{2(K-1)}$, which is attainable only if $K \leq 2M^2 + 1$. This is the Grassmannian Rankin bound for $T = 2M$.

References

[1] "Final report on the METIS 5G system concept and technology roadmap," Apr 2015.

[2] L. Zheng and D. N. Tse, "Communication on the grassmann manifold: A geometric approach to the noncoherent multiple-antenna channel," *Information Theory, IEEE Transactions on*, vol. 48, no. 2, pp. 359–383, 2002.

[3] R. H. Gohary and T. N. Davidson, "Noncoherent mimo communication: Grassmannian constellations and efficient detection," *Information Theory, IEEE Transactions on*, vol. 55, no. 3, pp. 1176–1205, 2009.

[4] D. Argawal, T. Richardson, and R. Urbanke, "Multiple-antenna signal constellations for fading channel," *IEEE Transactions on Informatiion Theory*, vol. 47, pp. 2618–2626, 2001.

[5] W. Zhao, G. Leus, and G. B. Giannakis, "Orthogonal design of unitary constellations for uncoded and trellis-coded noncoherent space-time systems," *Information Theory, IEEE Transactions on*, vol. 50, no. 6, pp. 1319–1327, 2004.

[6] Y. Jing and B. Hassibi, "Unitary space-time modulation via cayley transform," *Signal Processing, IEEE Transactions on*, vol. 51, no. 11, pp. 2891–2904, 2003.

[7] I. Kammoun, A. M. Cipriano, and J. C. Belfiore, "Non-coherent codes over the grassmannian," *Wireless Communications, IEEE Transactions on*, vol. 6, no. 10, pp. 3657–3667, 2007.

[8] A. Edelman, T. A. Arias, and S. T. Smith, "The geometry of algorithms with orthogonality constraints," *SIAM journal on Matrix Analysis and Applications*, vol. 20, no. 2, pp. 303–353, 1998.

[9] I. S. Dhillon, J. R. Heath, T. Strohmer, and J. A. Tropp, "Constructing packings in grassmannian manifolds via alternating projection," *Experimental mathematics*, vol. 17, no. 1, pp. 9–35, 2008.

[10] J. H. Conway, R. H. Hardin, and N. J. Sloane, "Packing lines, planes, etc.: Packings in grassmannian spaces," *Experimental mathematics*, vol. 5, no. 2, pp. 139–159, 1996.

[11] R. A. Rankin, "The closest packing of spherical caps in n dimensions," in *Proceedings of the glasgow mathematical association*, vol. 2, no. 03. Cambridge Univ Press, 1955, pp. 139–144.

[12] T. Ericson and V. Zinoviev, *Codes on Euclidean spheres*. Elsevier, 2001, vol. 63.

[13] M. Brehler and M. K. Varanasi, "Asymptotic error probability analysis of quadratic receivers in rayleigh-fading channels with applications to a unified analysis of coherent and noncoherent space-time receivers," *Information Theory, IEEE Transactions on*, vol. 47, no. 6, pp. 2383–2399, 2001.